Effects of Maleic Anhydride-Grafted Polypropylene (MAPP) on the Physico-Mechanical Properties and Rheological Behavior of Bamboo Powder-Polypropylene Foamed Composites

Xiaxing Zhou,[a] Yan Yu,[b] Qiaojia Lin,[a] and Lihui Chen [a,]*

To improve the interfacial compatibility between bamboo powder and polypropylene (PP), the effects of maleic anhydride-grafted polypropylene (MAPP) on the physico-mechanical properties and rheological behavior of 33 wt% bamboo powder/PP foamed composites were investigated. The results showed that the mechanical properties, water resistance, and surface wettability of MAPP-treated composites improved significantly, and the optimum content of MAPP was 9%. The density of 9% MAPP-treated composite was 0.845 g/cm^3 and its specific bending and tensile and notched impact strengths increased by 22.9%, 29.6%, and 49.0%, respectively, and the water absorption decreased from 8.80% to 1.92%, compared to the untreated composite. The frequency sweep results indicated that both the modulus and complex viscosity of the 9% MAPP-treated composite reached minimum values, and the slope of the lg*G′*-lg*f* curve for the treated composite increased by 15.9% compared with that of the untreated analogue. ESEM results indicated that the MAPP-treated composite had better bamboo powder dispersion and better interfacial compatibility. FTIR and XPS analyses confirmed the esterification between anhydride groups of MAPP and hydroxyl groups of bamboo powder. XRD studies showed the degree of crystallinity for the MAPP-treated composite increased to 26.52%, compared to 21.05% for the untreated composite.

Keywords: Bamboo powder-polypropylene foamed composite; MAPP; coupling agent; Physico-mechanical properties; Rheological behavior

*Contact information: a: College of Material Engineering, Fujian Agriculture and Forestry University, Fuzhou 350002, P. R. China; b: International Center for Bamboo and Rattan, Beijing 100102, P. R. China; * Corresponding author: lihuichen@263.net*

INTRODUCTION

China has the longest cultivation history of bamboo and the most abundant bamboo resources in the world. It is well known that bamboo fiber can be a renewable and cheaper substitute for synthetic fibers in some application fields, because of properties such as its low cost, high tensile modulus, sustainability, and biodegradability. Moreover, compared to wood, bamboo can renew itself much more rapidly, and the maturity time needed for bamboo is only three to four years, which is far less than the time needed for most woods. Due to these excellent properties, bamboo has attracted worldwide attention as a potential reinforcement for wood-plastic composites (WPCs) (Okubo *et al*. 2004). As the processing residue of bamboo, bamboo powder can also be suitable as reinforcement for WPCs.

WPCs have environmental and economic advantages for numerous applications in fields such as decoration, packing, building, and the automobile industry (Clemons 2002). To reduce the density and enhance the specific strengths of WPC and thus to broaden its application fields, the concept of introducing a uniform cellular structure into the WPC has recently been successfully demonstrated. Thermoplastics such as polypropylene (PP), polyethylene (PE), and polyvinyl chloride (PVC) are the main matrix materials used for foamed WPCs. However, PVC foamed products pollute the surrounding environment and pose problems during processing, use, and disposal; and thus they are used less than polyolefin-based foamed WPCs and most likely will be gradually abandoned. PE exhibits worse performance than PP in terms of mechanical strengths and heat resistance and is more difficult to degrade. Therefore, preparation of bamboo powder/PP foamed composites can be considered as a promising route to achieve a balanced property profile. Moreover, PP-based foamed WPCs have captured more attention at home and abroad recently, and there have been reports of some progress (Zhang *et al.* 2005; Bledzki *et al* 2005; Bledzki and Omar 2006a,b; Faruk *et al* 2007; Lee 2008; Ardanuy *et al.* 2012; Zhang *et al* 2012). The research interest is primarily focused on the effects of the type and concentration of foaming agents, reinforcements, additives, and coupling agents on the mechanical and physical properties and foamability of the foamed composites.

However, bamboo powder is hydrophilic and is inherently incompatible with hydrophobic PP (Zita Dominkovics *et al.* 2007). The poor interfacial bonding between the bamboo powder and PP can cause problems during the processing and also with respect to the mechanical properties of the resulting composites. Additionally, the formed hydrogen bonds between the hydrophilic fibers easily cause the bamboo powders to agglomerate into bundles, thus distributing the bamboo powders unevenly throughout the matrix during processing. To address these limitations, in recent years, natural fibers have been chemically modified to reduce their hydrophilic character, primarily with the methods of esterification, etherification, and benzylation (Freire *et al.* 2006), or by using coupling agents. In PP-based WPCs, MAPP and MAPE (Biplab *et al*. 2010; Deka and Maji 2010; Gao *et al*. 2012) and silane (Xie *et al*. 2010) are the most commonly reported and used coupling agents. However, studies concerning the effects of coupling agents on the properties of bamboo powder (BP)/PP foamed composites are relatively few, and only the effects of coupling agents on the mechanical properties of composites have been reported. In this study, the effects of various contents of MAPP on the physico-mechanical properties, water resistance, and rheological behavior of the BP/PP foamed composites were investigated to obtain the BP/PP foamed composite with the highest strength-to-weight ratio and optimal rheological behavior. Additionally, the interfacial bonding mechanism was explored using ESEM, FTIR, XPS, and XRD.

EXPERIMENTAL

Materials

Polypropylene (PP) (type K8303) with a density of 0.90 g/cm^3, a melting index (MI) of 2.4 g/10 min at 230 °C, 2.16 KN, and a melting temperature of 168 °C was provided from ExxonMobil Chemicals. High melt strength polypropylene (HMSPP) (type SMS-514F) with a density of 0.91 g/cm^3, a MI of 3.2 g/10 min at 230 °C, 2.16 KN, and a melting temperature of 175 °C from Korea Honam Petrochemical Ind. Co. was

used. Moso bamboo (*Phyllostachys edulis*) powder with a density of 1.37 g/cm^3 and with a mixture of particle sizes in the range of 90 to 450 μm was supplied by Zhejiang Lin-an Mingzhu Bamboo & Wood Industry Co., Ltd, China. The exothermic foaming agent (FA) azodicarbonamide (AC) with gas evolution of 240 mL/g was obtained from Shanghai Jieyu Industry and Trading Co. Ltd, China, and the AC was modified by nano-ZnO (size 40 nm) and $Zn(St)_2$ complex; the ratio of AC:ZnO:$Zn(St)_2$ was 100:10:10. To improve the interfacial compatibility between the bamboo powder, PP, and HMSPP, a maleic anhydride grafted polypropylene (MAPP) coupling agent from Nanjing Deba Chemical Co. Ltd, China was used. Five proportions of MAPP, *i.e.*, 0%, 3%, 6%, 9%, and 12 wt% of bamboo powder, were studied in this research.

Processing

First, bamboo powder was dried in an oven at 100 °C for 10 h. Then, PP and HMSPP with MAPP, a lubricant, and dried BP were mixed in a high-speed mixer (Henschel Mixer, type HM40 KM120) for 10 min. Second, the mixture was transferred to mix in a HAKKE mixer at 180 °C with a rotational speed of 40 rpm for 12 min. After that, the blends were crushed into granules for injection moulding in a WSGM-250 mill. Finally, the FA and BP/PP granules were mixed, and foamed samples were prepared using an injection machine at a melting temperature of 160 to 190 °C, a mould temperature of 90 °C, an injection pressure of 5 to 6 MPa, a packing pressure of 4 MPa, and a packing time of 10 s. The PP accounted for 53 wt%, the HMSPP accounted for 13 wt%, the BP accounted for 33 wt%, and the FA accounted for 1 wt% of the foamed composites. This ratio was used because previous studies reported that the comprehensive mechanical properties of foamed composites were best when the amount of BP was 33 wt% (Zhou *et al*. 2012).

Measurements

Physico-mechanical properties

The densities of foamed specimens were measured according to ASTM D792. The flexural properties in three-point bending mode and the tensile strength were respectively measured in accordance with ASTM D790 and ASTM D638 at a crosshead speed of 10 mm/min. The notched impact strength and the vicat softening point (VST) tests were performed following ISO 8256-2005 and ASTM D1525-2000, respectively. Multiple measurements (7 runs) were conducted for all tests, and mean values are reported. A universal testing machine (CMT6000, Shenzhen SANS, China) was used.

Water absorption and thickness swelling

Percentage water absorption and thickness swelling were measured following ASTM D570-2005 procedure. The foamed pallets were submerged in a distilled water-filled container at 23 °C for 1440 h. All values were calculated as the mean of 3 samples. The water absorption (WA) and thickness swelling (TS) were respectively determined as,

$$WA = \left(\frac{m_t - m_o}{m_o}\right) \times 100 \quad (1)$$

where m_t is the mass of the sample after water soaking and m_o is the mass of the sample before water soaking; and,

$$TS = (\frac{T_t - T_o}{T_o}) \times 100 \quad (2)$$

where T_t is the thickness of the sample after water soaking and T_o is the thickness of the sample before water soaking.

Surface dynamic wettability

The contact angles of foamed specimens with dimension of 30 mm (length) × 12 mm (width) × 4 mm (thickness) were measured using a contact angle goniometer (JC2000A, Shanghai, China). A drop of reagent was placed on the composite surface; two kinds of pure test liquids, *i.e.*, distilled water and glycerin, were used. Experiments were conducted measuring the contact angle as a function of time; the measurements were carried out for 300 s, and the recorded points were 0 s, 5 s, 10 s, 20 s, 30 s, 40 s, 60 s, 80 s, 100 s, 130 s, 160 s, 190 s, 220 s, 260 s, and 300 s. The experimental contact angle data are the mean values of five time measurements. In addition, the dynamic wettability model was used to characterize the contact angle with the following equation,

$$\theta = \theta_e + A\exp(-Kt) \quad (3)$$

where θ is contact angle at time t, θ_e represents the equilibrium contact angle, A is an integral constant, and K is a constant that refers to the intrinsic relative decrease rate of the contact angle and can be used to evaluate the wettability of composites.

The surface free energy of composites can be obtained according to the formulas for the surface free energy and the contact angle,

$$\gamma_{l1}(\cos\theta_1 + 1) = 2(\gamma_s^{\ D}\gamma_{l1}^{\ D})^{1/2} + 2(\gamma_s^{\ P}\gamma_{l1}^{\ P})^{1/2} \quad (4)$$

$$\gamma_{l2}(\cos\theta_2 + 1) = 2(\gamma_s^{\ D}\gamma_{l2}^{\ D})^{1/2} + 2(\gamma_s^{\ P}\gamma_{l2}^{\ P})^{1/2} \quad (5)$$

$$\gamma_s = \gamma_S^{\ D} + \gamma_S P \quad (6)$$

where θ_1 and θ_2 are the contact angles of composites using water and glycerin as reagents, respectively, γ_s is the surface free energy of the solid composite, γ_s^D and γ_s^P are the non-polar and polar component of the surface free energy, γ_{l1} and γ_{l2} are the surface free energy of water and glycerin, respectively, γ_{l1}^D and γ_{l1}^P are 21.8 mJ·m^{-2} and 51 mJ·m^{-2} , respectively; and γ_{l2}^D and γ_{l2}^P are 37 mJ·m^{-2} and 26.4 mJ·m^{-2}, respectively.

Rheological behavior

The rheological behaviors of samples with diameters of 30 mm and thicknesses of 2.2 mm were investigated with a rotary rheometer (Haake ARSⅢ, Germany). A dynamic frequency sweep test was conducted to measure the storage modulus (G'), loss modulus (G''), and complex viscosity (η^*) in a frequency range from 0.1 to 100 Hz. The dynamic viscoelastic measurement was done in the linear viscoelastic region at a constant temperature of 180 °C.

ESEM analysis

The tensile fractured surfaces of untreated and MAPP-treated composites were investigated using an environmental scanning electron microscope (ESEM, PHILIPS XL30, FET, Netherlands) after being sputtered with gold.

FTIR studies

FTIR spectra of BP, MAPP, MAPP-treated BP, composites and MAPP-treated composite were recorded with a FTIR device (AGL0702005 Nicolet 380, USA) at test conditions of 4 cm^{-1} resolution, scan number of 32, and scan range of 4000 to 400 cm^{-1}. The samples were mixed with KBr at a ratio of approximately 1:20.

XPS analysis

The compositions of composites, both untreated and MAPP-treated, were analyzed using an X-ray photoelectron spectroscope (XPS, type ESCALLAB 250, UK) with a scientific theta probe. Three types of spectra were collected: a survey spectrum, a high-resolution spectrum of the C1s region, and a high-resolution spectrum of elemental O.

To determine the types of oxygen-carbon bonds present, chemical bond analysis of carbon was accomplished by curve fitting the C1s peak and deconvoluting it into four subpeaks. Meanwhile, the oxygen peak was divided into two subpeaks according to a previous report by Inari *et al*. (2006). The deconvoluted peak assignments of C1s and O1s with their corresponding bond types are listed in Table 1. The ratio of oxygenated to unoxygenated carbon ($C_{ox/unox}$) was calculated according to (Dorris and Gray 1978):

$$C_{ox/unox} = \frac{C_{oxygenated}}{C_{unoxygenated}} = \frac{C2 + C3 + C4}{C1} \quad (7)$$

Table 1. Deconvoluted Peak Assignments for Carbon and Oxygen Elements

Carbon Group	Bond Type	Oxygen Group	Bond Type
C1	C-C or C-H	O1	C=O
C2	C-O		
C3	O-C-O or C=O	O2	C-O
C4	O-C=O		

X-Ray Diffraction Analysis

The supermolecular structures of untreated and MAPP-treated composites were investigated using X-ray diffraction (XRD). The XRD data were obtained using a Japan MiniFlex2 instrument, and the samples were prepared as powder. Ni-filtered Cu-Kα radiation generated at a voltage of 30 kV and current of 15 mA was utilized. The scanning angle range was 5° to 80° with a scan speed of 4 °/min. To calculate the crystallinity, MDI Jade software was applied.

RESULTS AND DISCUSSION

Effects of MAPP Content on the Physico-Mechanical Properties of Composites

Physico-mechanical properties

Figure 1 shows the influence of MAPP content on the physico-mechanical properties of BP/PP foamed composites. A significant improvement in mechanical properties was achieved using MAPP as a coupling agent for composites. As can be seen, the mechanical properties and VST were enhanced at first and then decreased as the MAPP content was further increased. The specific flexural and tensile strengths were significantly increased with the addition of 3% MAPP and then continuously slightly increased until the MAPP content reached up to 9%. The flexural modulus and specific notched impact strength improved steadily as the MAPP content was increased and decreased obviously when the MAPP content exceeded 9%. That is, when 12% MAPP was used, the mechanical properties decreased, especially the notched impact strength, and the VST also was reduced slightly. Thus, higher MAPP contents did not lead to better performance, and the optimum amount of MAPP was considered to be 9%.

The density of 9% MAPP-treated composite decreased to 0.845 g/cm^3, which is an decrease of 15% compared with that of the unfoamed composite (0.994 g/cm^3) (Zhou *et al*. 2012). Also the flexural modulus and the specific flexural, tensile, and notched impact strengths of 9% MAPP-treated composite reached maximum values of 2.91 GPa, 47.59 MPa, 26.60 MPa, and 7.45 KJ/m^2, respectively, yielding improvements of 6.0%, 22.9%, 29.6%, and 49.0%, respectively, compared to the untreated composite. Additionally, when the MAPP content was 9%, the VST was slightly enhanced, increasing from 153.5 °C to 155.4 °C, suggesting that the thermal stability of MAPP-treated composites improved to some extent. This may be ascribed to the reduction in heat motion of the matrix molecules because of the modified bamboo powder. The increased VST data also indicated that the rigidity of the treated composite was enhanced.

The improvement in mechanical strength may be attributed to the hydrophilic anhydride groups of MAPP, which are prone to compatibilizing with hydrophilic bamboo powder particles, thereby promoting the dispersion and surface wetting of bamboo powder particles in the matrices (Fig. 5).

In addition, anhydride groups can react with the hydroxyl groups of bamboo powder and form ester bonds, improving the interfacial adhesion between the matrices and fillers (Gao *et al*. 2012). Moreover, the interfacial compatibility among PP, HMSPP, and BP was improved, which could lead to the efficient transfer of stress from the matrices to the stiffer bamboo powders and thus enhance the mechanical strength (Herrera-Franco and Valadez-González 2005; Lu *et al*. 2005).

However, at a higher MAPP concentration (12%), the excessive MAPP may form a layer of macromolecules, resulting in decreased uniformity between the fillers and matrices and leading to decreased interfacial adhesion. Furthermore, adding redundant MAPP may cause increased radical depolymerization of the plastic molecules, thereby leading to the reduction of the notched impact strength.

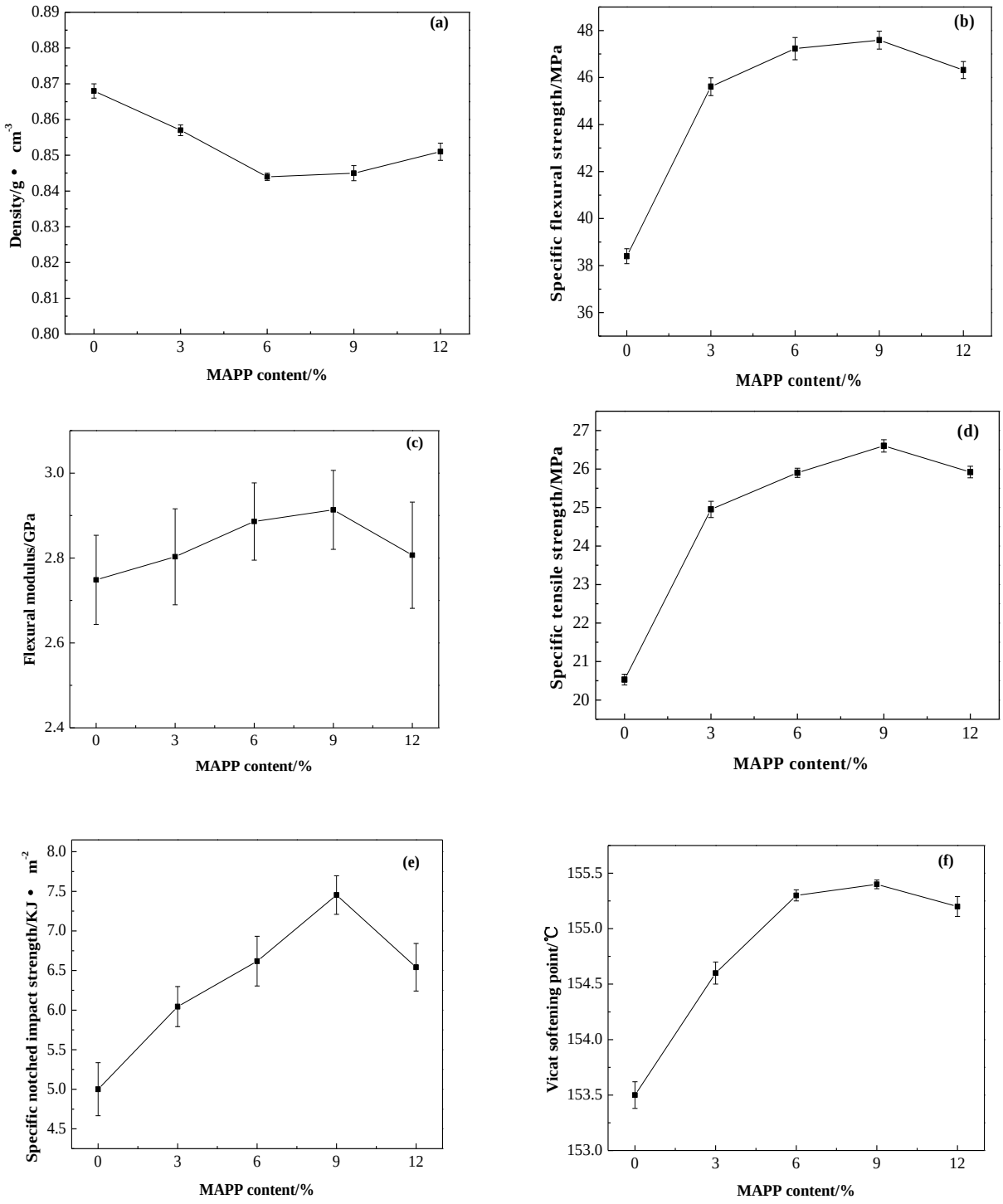

Fig. 1. Influence of MAPP content on the physico-mechanical properties of foamed composites: (a) density, (b) specific flexural strength, (c) flexural modulus, (d) specific tensile strength, (e) specific notched impact strength, and (f) vicat softening point. Note: Specific strength was calculated from the ratio of strength to its specific density that is the material's strength divided by its density.

Water absorption and thickness swelling

The time dependences of water absorption (WA) and thickness swelling (TS) for composites with different MAPP contents are shown in Fig. 2. In all cases, WA and TS exhibited nearly proportional increases with increasing immersion time during the first 720 h, and then WA and TS increased at a slower rate after 720 h. It was found that the WA and TS of composites were considerably reduced due to the addition of MAPP. The WA and TS for the untreated composite were 8.80% and 1.85%, respectively, after an immersion time of 1440 h. This can be ascribed to the poor interface between fillers and matrices. With increasing MAPP content, WA and TS were markedly reduced and the growth trend of WA and TS was significantly decreased. The WA and TS of the 9% MAPP-treated composite eventually reduced to final constant values of 1.92% and 1.13%, respectively. These results clearly revealed that the use of MAPP coupling agent had a beneficial effect on the WA and TS of the composites. This may be explained, first, by the promoted dispersion of bamboo powder in the plastic matrices and by the improved interfacial adhesion between the bamboo powder particles and matrices. Second, these results may have occurred because the improved interfacial adhesion slowed down the water diffusion rate between the bamboo powder particles through interfacial defects (Xie *et al*. 2010). Last but not least, the reduced amount of hygroscopic hydroxyl groups in the bamboo polymers due to the esterification with anhydride groups contributed to the reduced water uptake and thickness swelling. However, the composite with a higher MAPP content (12%) exhibited a smaller water uptake and thickness swelling than that modified with 9% MAPP. This observation may be attributed to the increased amount of non-reacted MAH.

Based on a comprehensive consideration of the physico-mechanical properties and water resistance, the most suitable amount of MAPP was judged to be 9%. Such excellent properties allow the foamed composite to be used in many industrial applications, such as decoration, building and packing materials, and automotive interior parts.

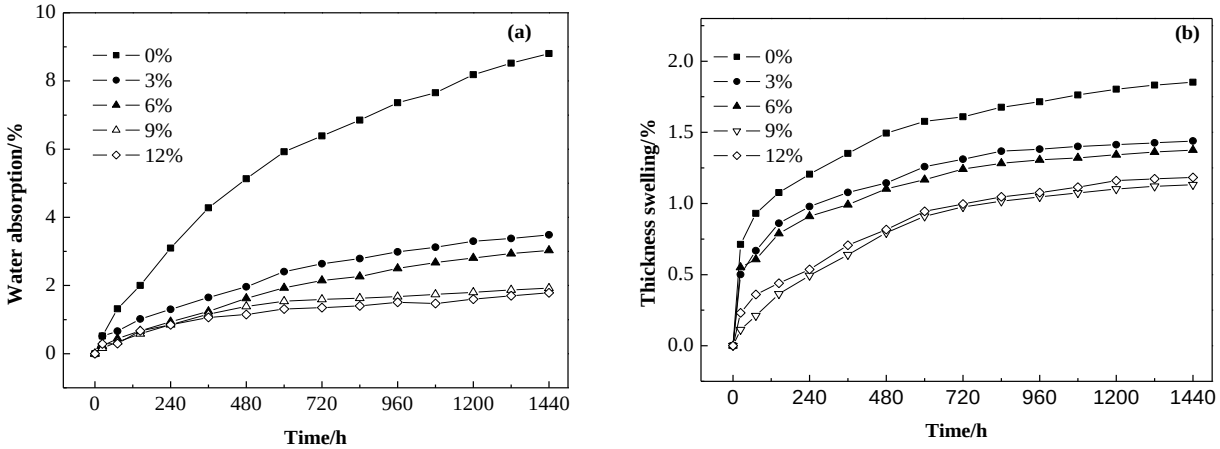

Fig. 2. Influence of MAPP content on the water absorption and thickness swelling of foamed composites: (a) water absorption and (b) thickness swelling

Dynamic surface wettability

Figure 3 and Table 2 represent the dynamic surface wettability of the untreated and 9% MAPP-treated composites. At the initial stage of the wetting process, the contact angle decreased quickly. As time elapsed, the contact angle decreased more slowly and

reached an equilibrium value after 300 s. The wetting model as mentioned in Eq. (3) could simulate the surface wettability well, and the correlation coefficients R^2 were all over 0.96. This mathematical expression has also been used to successfully characterize the wettability of other wooden materials (Wei *et al*. 2012 and Xu *et al*. 2012). After fitting the model, the contact angle curves and *K* values were calculated. MAPP played an effective role in improving the surface wettability of composites. The *K* values of the untreated composite were 0.0034 and 0.0065 when using water and glycerin, respectively. With the addition of 9% MAPP, the treated composite exhibited greater *K* values (0.0071 and 0.0119, respectively) than the untreated composite.

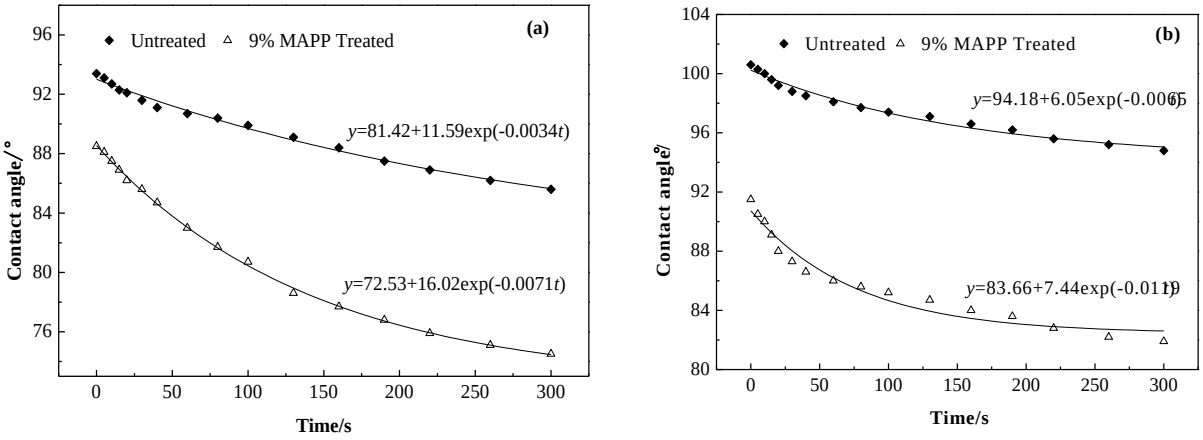

Fig. 3. Influence of MAPP on the dynamic surface wettability of foamed composites: (a) using water as reagent and (b) using glycerin as reagent

Table 2 shows that the initial and final contact angles of the MAPP-treated composite were much lower than those of the untreated one. Meanwhile, the treated composite showed higher surface free energy (34.19 $mJ \cdot m^{-2}$) than the untreated one (28.02 $mJ \cdot m^{-2}$). Therefore, the surface wettability of the MAPP-treated composite improved and thus contributed to the enhancement of the post-processing performance of composites.

Table 2. Effects of MAPP on the Surface Wettability of Foamed Composites

Sample	Reagent	Contact angle/°		*K*	Correlation Efficient R^2	Polar Free Energy /$mJ \cdot m^{-2}$	Non-Polar free Energy /$mJ \cdot m^{-2}$	Surface Free Energy /$mJ \cdot m^{-2}$
		Initial Value	Final Value					
Untreated	Water	93.4	85.6	0.0034	0.992	0.09	27.92	28.02
	Glycerin	100.6	94.8	0.0065	0.982			
9% MAPP Treated	Water	88.5	74.5	0.0071	0.999	1.19	33.00	34.19
	Glycerin	91.5	81.9	0.0119	0.964			

Effects of MAPP Content on the Rheological Behavior of Composites

The effects of adding different contents of MAPP on the storage modulus (*G*') and loss modulus (*G*") as a function of frequency (*f*) are presented in Fig. 4 (a) and (b). The modulus of the composites exhibited a linear increase with increasing frequency (*f*).

Compared to the untreated composite, the storage modulus and loss modulus were first reduced with the addition of MAPP, reached a minimum when the MAPP content was 9%, and then increased with the addition of 12% MAPP. This is because, with the addition of MAPP, the interfacial bonding of bamboo powders and matrices improved and thus the modulus was enhanced. Also, after MAPP modification, the surface of the bamboo powder was well coated by the matrices and therefore the modulus of the composites were reduced. Moreover, the thermoplastic behavior of treated composites was increased after esterification and thereby the modulus of the composites was reduced. These two effects existed simultaneously, and both played a dominant role at various times (Ou *et al*. 2009). Through linear fitting of the lgG'-lg$f$ curve at low frequencies, the slopes of the untreated sample and samples with 3%, 6%, 9%, and 12% MAPP were 0.709, 0.746, 0.782, 0.822, and 0.796, respectively. The coefficients of determination were over 0.98. The available research showed that the higher the slope (as calculated using the above method), the greater the homogeneous phase of the composite (Gao *et al*. 2008). Therefore, the increase in the slopes of lgG'-lg$f$ indicated that the degree of homogeneity of all treated composites increased and that the homogeneity for the 9% MAPP composite was highest. This result corresponds to the mechanical tests.

Figure 4 (c) shows the frequency dependence of the loss tangent (tanδ). The tanδ value has been associated with gel-like structures, which in turn indicates the interaction between melt and particles (Chambon and Winter 1987). In frequency ranges of about 0.1 to 1.5 Hz, both untreated and MAPP-treated composites showed liquid viscoelastic behavior ($G''>G'$), which was not seen in the 1.5 to 100 Hz range. This is because, at low frequencies, most of the deformation was from the viscous flowing, and as the frequency increased, the disentangled speed of molecular chains was faster than the entangled one, so the growth rate of the storage modulus was greater than that of the loss modulus. Meanwhile, at higher frequencies, the relaxation time of the polymer shortened and more energy was released by the stored polymer deformation; thus, the composite showed high flexibility.

Figure 4 (d) shows the complex viscosity (η^*) versus f for samples with different percentages of MAPP. The η^* was decreased substantially with an increase of f, and all samples showed shear thinning behavior (Yokozeki *et al*. 2012). Compared to the untreated composite, a subtle reduction in complex viscosity was observed for composites with additions of 3%, 6%, and 9% MAPP. On the contrary, the complex viscosity of the 12% MAPP-treated composite was higher than that of the untreated analogue. The reason for this phenomenon was the same as that given for the variation of modulus. This result confirmed that the flowing behavior of the 9% MAPP-treated composites was enhanced.

Effect of MAPP on Fracture Morphology

The tensile fracture morphology of specimens was investigated using an ESEM, and the results are presented in Fig. 5. Figure 5(a) reveals that the interfacial adhesion between the fillers and the matrices of PP and HMSPP was poor and the fractured surface exhibited many voids, while the interface between the bamboo powders and matrices was considerably clearer. Meanwhile, it was observed that some bamboo powder particles agglomerated into bundles and were unevenly distributed throughout the matrices; these defects caused stress concentrations and contributed to the lower mechanical strength of the untreated composites compared to those of the treated composites. Furthermore, in

some parts, there were no matrices coating the bamboo powder surface or holes made by bamboo powder being pulled out of the matrices during the tensile stress failure.

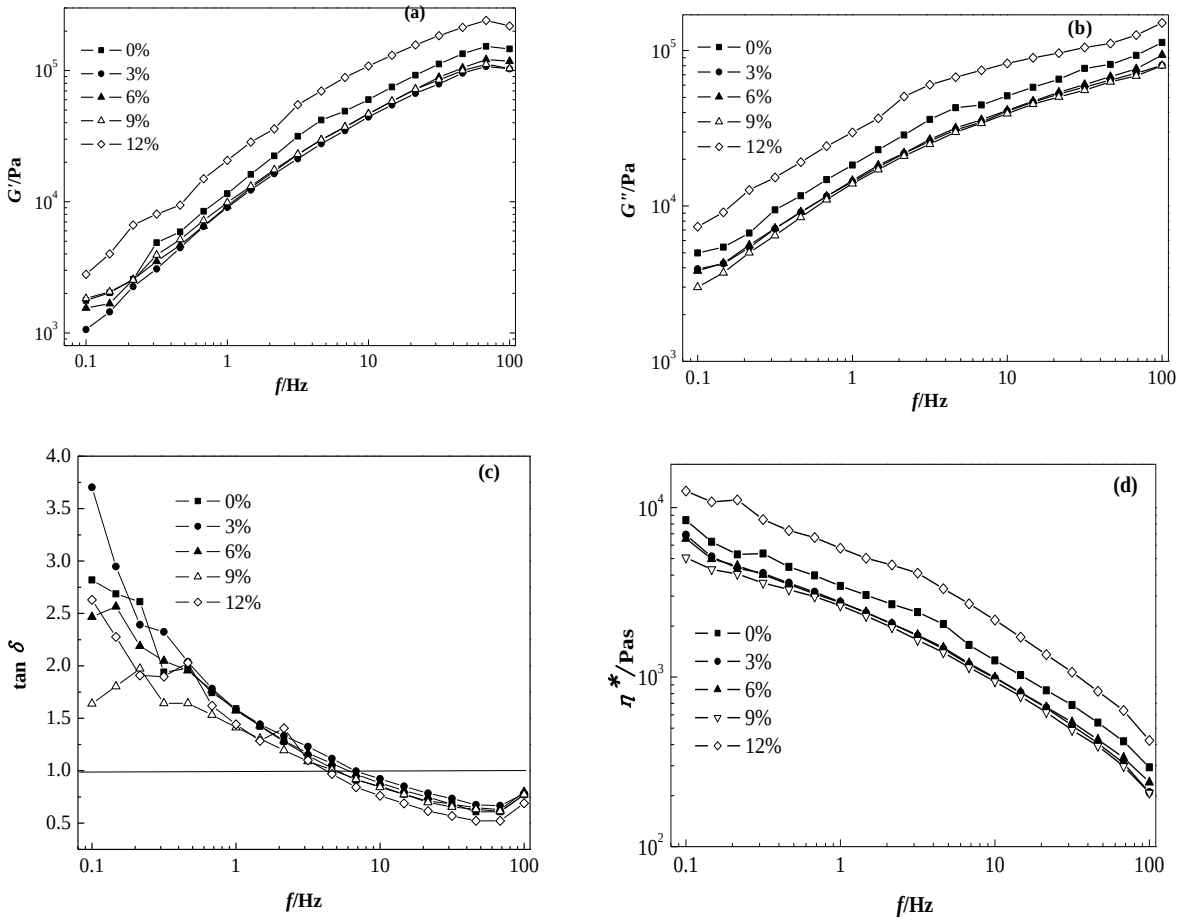

Fig. 4. The frequency dependence of dynamic viscoelastic functions for composites with different MAPP contents at 180 °C

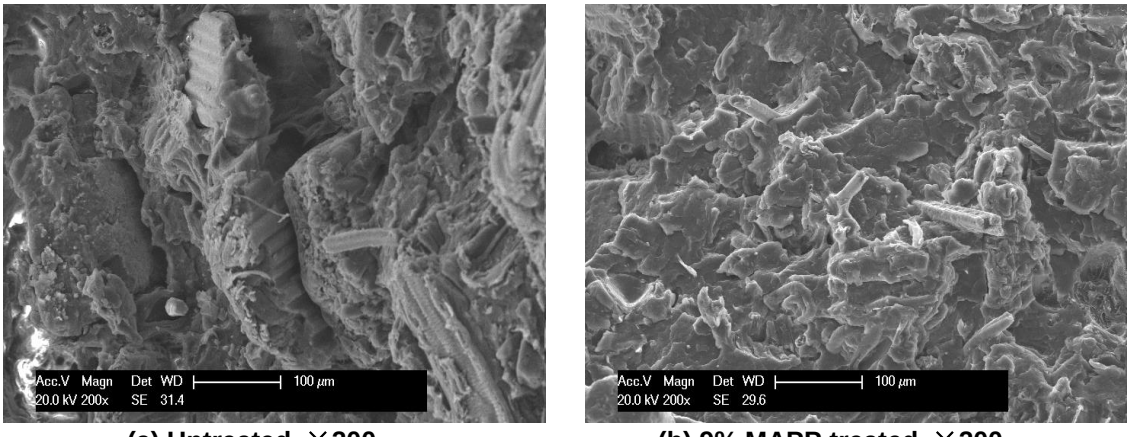

(a) Untreated ×200 **(b) 9% MAPP treated ×200**

Fig. 5. Cell structure of bamboo powder/PP foamed composites: a) untreated and b) 9% MAPP-treated

As can be seen in Fig. 5(b), after modification by 9% MAPP, the compatibility between fillers and matrices was improved, the interfacial boundary became indistinct, and the distribution of bamboo powder was improved. This result further confirmed that MAPP can improve the interfacial compatibility of BP/PP foamed composites.

FTIR Study

FTIR spectra of MAPP, BP, MAPP-treated BP, untreated composites, and MAPP-treated BP/PP foamed composites are shown in Fig. 6. In the MAPP spectrum (Fig. 6a), the absorption peak at 3537 cm^{-1} was for –OH stretching; the peaks at 2960 cm^{-1}, 2922 cm^{-1}, and 1461 cm^{-1} were assigned to asymmetric, symmetric, and scissor modes of -CH stretching, respectively; and the characteristic peak at 1740 cm^{-1} was assigned to C=O stretching. The FTIR spectrum of untreated BP (Fig. 6b) showed the presence of bands at 3402 cm^{-1} for –OH stretching, 2915 cm^{-1} for -CH stretching, 1601 cm^{-1} and 1510 cm^{-1} for C=C aromatic ring, 1424 cm^{-1} for $–CH_2$ deformation in lignin and carbohydrates, and 1051 cm^{-1} for C-O stretching. The MAPP-treated BP (Fig. 6c) exhibited new peaks at 2952 cm^{-1} and 2838 cm^{-1} for -CH stretching and 1738 cm^{-1} for C=O stretching, which confirmed the esterification reaction between the hydroxyl group of BP and the anhydride of MAPP; the frequencies at 3402 cm^{-1}, 2915 cm^{-1}, 1601 cm^{-1}, 1510 cm^{-1}, 1424 cm^{-1}, and 1051 cm^{-1} were correspondingly shifted to 3424 cm^{-1}, 2920 cm^{-1}, 1604 cm^{-1}, 1513 cm^{-1}, 1461 cm^{-1}, and 1034 cm^{-1} in the MAPP-treated BP spectrum due to the incorporation of MAPP. Figures 6 (d) and (e) show the FTIR spectra of untreated and 9% MAPP-treated composites. In the MAPP-treated composite, new peaks appeared at 1726 cm^{-1} for carbonyl (C=O) stretching and at 2957 cm^{-1} and 2839 cm^{-1} for –CH stretching of the modifying hydrocarbon; the intensity of -OH stretching decreased and shifted from 3429 cm^{-1} (Fig. 6d) to 3403 cm^{-1} (Fig. 6e); and the intensity of C-O stretching increased and shifted from 1049 cm^{-1} (Fig. 6d) to 1063 cm^{-1} (Fig. 6e).

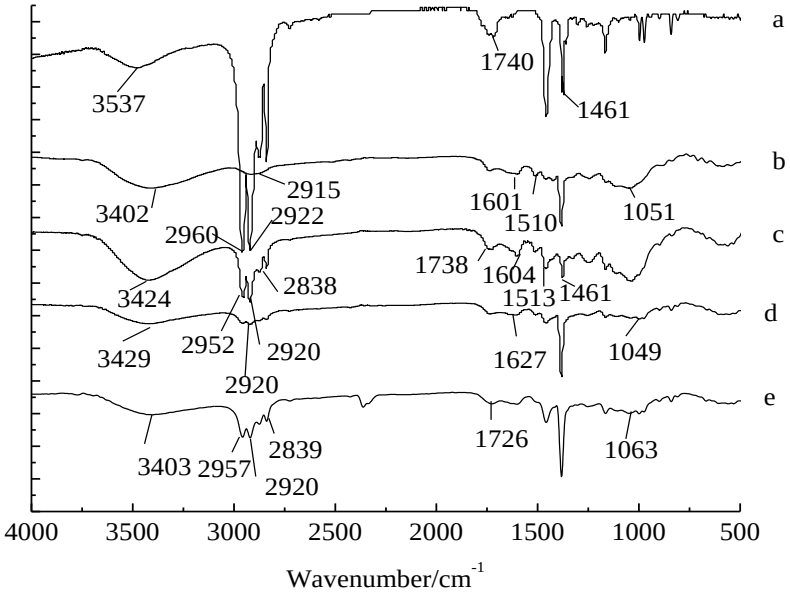

Fig. 6. FTIR spectra of bamboo powder and bamboo powder/PP foamed composites: (a) MAPP, (b) untreated bamboo powder, (c) MAPP-treated bamboo powder, (d) untreated composite, and (d) MAPP-treated composite

The results shown in Fig. 6 demonstrate that MAPP underwent an esterification reaction or hydrogen bonding between the hydroxyl groups of the bamboo powder on one side and the carboxylic groups of the MAPP diffused matrices on the other side. Such interactions explain why the MAPP enhanced the interfacial bonding between BP and PP, improving the properties of the composites.

XPS Analysis

The carbon and oxygen XPS spectra for composite surfaces before and after 9% MAPP treatment are pictured in Figs. 7 and 8. The elemental composition and amount of different carbon-to-oxygen bonds on the foamed composite surfaces are shown in Table 3. With the addition of MAPP, the intensity of elemental C for the composite increased, and the content increased from 81.71% to 92.72%; on the contrary, the intensity and elemental content of O decreased. Both the untreated and MAPP-treated composites only contained three C1s bond types: primarily C1, followed by C2 and, finally, C3.

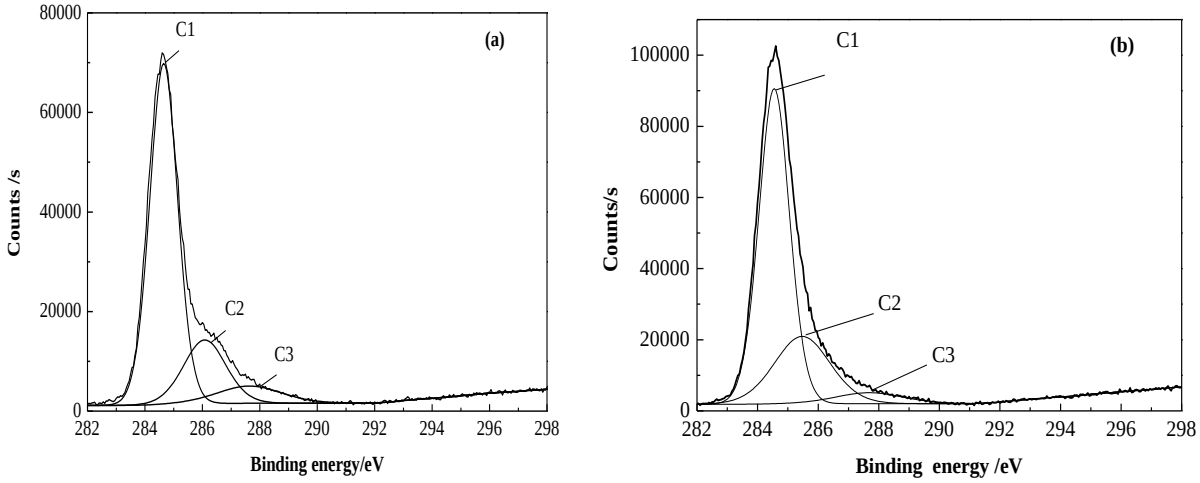

Fig. 7. Carbon XPS spectra of foamed composite surfaces: (a) untreated and (b) 9% MAPP-treated

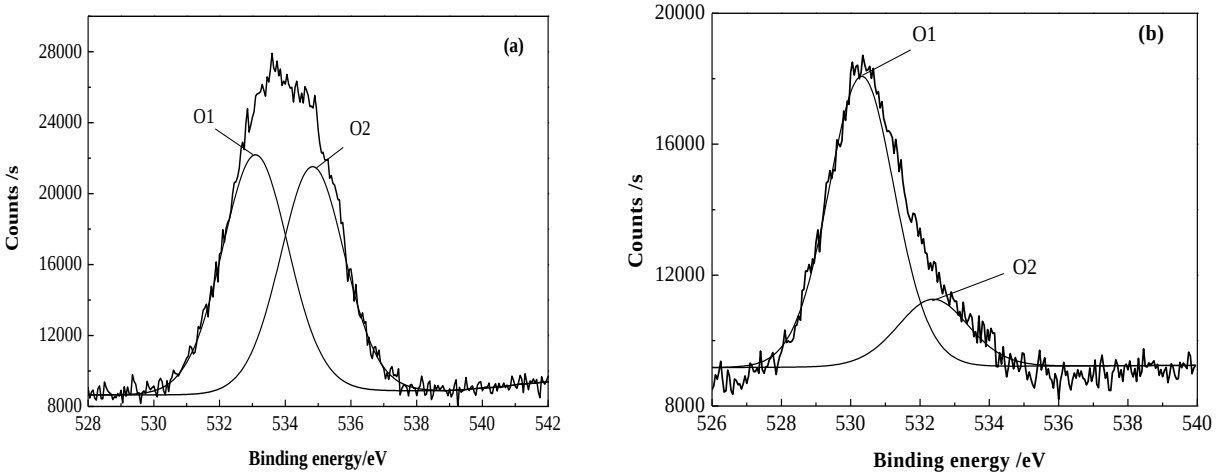

Fig. 8. Oxygen XPS spectra of foamed composite surfaces: (a) untreated and (b) 9% MAPP-treated

The XPS data listed in Table 3 reveal an increase in the amount of C1 and C2; as for the relative amount, only the C2, representing the C-O bond, increased; the C1 and C3 were slightly reduced for the MAPP-treated composite. The $C_{ox/unox}$ value for 9% MAPP-treated samples was higher than that of the untreated sample, with an increase from 0.40 to 0.47. In addition, the binding energy of C1s changed after MAPP modification, which indicated that the chemical structure of the composite changed. Table 3 also illustrates that there was an obvious decrease in the content of O2, representing C-O, relative to the O1 component of C=O. Additionally, from the peak areas, it was determined that the O1/O2 ratio was 1.09 for the untreated composite and 2.26 for the MAPP-treated composite. These results confirmed the chemical reaction of MAPP and bamboo powders. It has been reported that the relative content of O1 can be regarded as the area of crystallization; on the contrary, the relative content of O2 can be regarded as the amorphous area (Di and Gao 2010). Therefore, the results indicated that the crystallinity of the MAPP-treated composite increased to some extent. This result also can explain the enhancement of the physico-mechanical properties of the treated composite. Additionally, the increase in the number of the strongly polar group C=O for the MAPP-treated composite accounted for the improvement in its surface wettability.

Combined with the ESEM and FTIR results, it is clear that MAPP can both improve the dispersion of bamboo powders and enhance the interfacial capability of the BP/PP foamed composite.

Table 3. Elemental Composition and Relative Amount of Different Carbon-to-Oxygen Bonds at Foamed Composite Surfaces

Sample	Elemental Composition (%)							
	C1s				O1s			N1s
	C1	C2	C3	$C_{ox/unox}$	O1	O2	O1/O2	
Untreated	58.38	16.54	6.79	0.40	8.59	7.86	1.09	1.84
9% MAPP Treated	63.27	24.64	4.81	0.47	4.15	1.84	2.26	1.29

XRD Analysis

Figure 9 shows the XRD results of HMSPP, PP, BP, and the BP/PP composite both untreated and treated with 9% MAPP. The XRD data and crystallization properties of foamed composites before and after MAPP treatment are listed in Table 4. HMSPP (curve a) showed a diffraction peak at 2θ values of approximately 14.44° (110), 17.21° (040), 18.96° (130), and 22.06° (301). The peaks (curve b) appearing at 2θ~14.26°, 17.22°, 18.88°, and 21.96° were for the crystalline portion of PP. The diffraction peaks of bamboo powder (curve c) appeared at 2θ~14.8°, 16.8°, and 22.4°, which is the characteristic peak of cellulose I. In the diffractograms of the untreated composite (curve d), the most prominent peaks appeared at 2θ~14.19° (110), 17.01° (040), 18.76° (130), and 21.26° (301) for the crystalline portion of PP and HMSPP present in the blend; the sharp high peak that appeared at 2θ~22.08° was for the crystalline portion of bamboo powder. Figure 9 (e) represents the diffractograms of the 9% MAPP-treated composite. Compared to the untreated composite, the MAPP-treated composite exhibited the characteristics of α-crystalline for PP and cellulose I for bamboo powder. However, Table 4 shows that the calculated degree of crystallinity of the treated composite was 26.52%,

in contrast to 21.05% for the untreated composite. This result was consistent with the FTIR and XPS analysis.

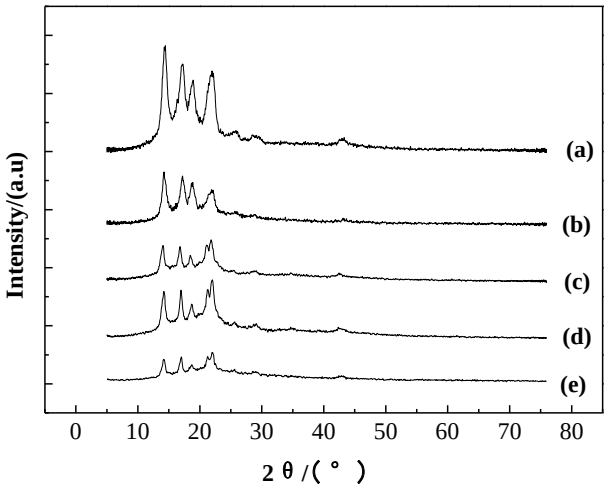

Fig. 9. X-ray diffraction patterns of (a) HMSPP, (b) PP, (c) bamboo powder, (d) the MAPP-treated composite, and (e) the untreated composite

Table 4. Crystallization Properties of Foamed Composites Before and After MAPP Treatment

Sample	2θ (°)					Crystallinity (%)
	I_{002}	I_{110}	I_{040}	I_{130}	I_{301}	
Untreated	22.076	14.186	17.009	18.756	21.262	21.05
9% MAPP Treated	21.966	14.137	16.921	18.780	21.331	26.52

CONCLUSIONS

1. The bamboo powder/PP foamed composite with the addition of 9% MAPP showed the best physico-mechanical properties, with an increase of 22.9% to 49.0% compared with the untreated composite. Additionally, the water resistant and surface wettability of the MAPP-treated composite improved, and the *K* value and the surface free energy were increased.
2. Frequency scan results showed that the modulus and complex viscosity for the 9% MAPP-treated composite reached a minimum, and the slope of a plot of lg*G′ versus* lg*f* in the low-*f* region increased from 0.709 to 0.822, which indicated that the flowing performance was enhanced and the homogeneity of the composite was improved.
3. ESEM, FTIR, and XPS results revealed that the interfacial compatibility of the MAPP-treated composite was improved.
4. XRD results revealed that the degree of crystallinity increased from 21.05% to 26.52% after modification with 9% MAPP.

ACKNOWLEDGMENTS

The authors gratefully acknowledge the generous financial support of the Twelfth Five-Year National Science and Technology Program "Research on Weather-resistant and Mould-proof Bamboo-Plastic Composites" (2012BAD54G01).

REFERENCES CITED

Ardanuy, M., Antunes, M., and Velasco, J. I. (2012). "Vegetable fibres from agricultural residues as thermo-mechanical reinforcement in recycled polypropylene-based green foams," *Waste Management* 32(2), 256-263.

Bledzki, A. K., Zhang, W. Y., and Omar, F. (2005). "Microfoaming of flax and wood fibre reinforced polypropylene composites," *Eur. J.Wood Wood Prod.* 63(1), 30-37.

Bledzki, A. K., and Omar, F. (2006a). "Microcellular injection molded wood fiber-PP composites: Part I - Effect of chemical foaming agent content on cell morphology and physico-mechanical properties," *Journal of Cellular Plastics* 42(1), 63-76.

Bledzki, A. K., and Omar, F. (2006b). "Microcellular injection molded wood fiber-PP composites: Part II - Effect of wood fiber length and content on cell morphology and physico-mechanical properties," *Journal of Cellular Plastics* 42(1), 77-88.

Chambon, F., and Winter, H. H. (1987). "Linear viscoelasticity at the gel point of a crosslinking PDMS with imbalanced stoichiometry," *J. Rheol.* 31(8), 683-997.

Clemons, C. (2002). "Wood-plastic composites in the United States - The interfacing of two industries," *Forest Prod. J.* 52(6), 10-18.

Deka, B. K., and Maji, T. K. (2010). "Effect of coupling agent and nanoclay on properties of HDPE, LDPE, PP, PVC blend and phargamites karka nanocomposite," *Composites Science and Technology* 70(12), 1755-1761.

Di, M., and Gao, Z. (2010). *Modern Analytical Techniques for Biomass Material*, Chemical Industry Press, Beijing.

Dominkovics, Z., Dányádi, L., and Pukánszky, B. (2007). "Surface modification of wood flour and its effect on the properties of PP/wood composites," *Composites: Part A* 38(8), 1893-1901.

Dorris, G. M., and Gray, D. G. (1978). "The surface analysis of paper and wood fiber by ESCA-electron spectroscopy for chemical analysis. Application to cellulose and lignin," *Cellulose Chemistry and Technology* 12, 9-23.

Faruk, O., Bledzki, A. K., and Matuana, L. M. (2007). "Microcellular foamed wood-plastic composites by different processes: A review," *Macromolecular Materials and Engineering* 292(2), 113-127.

Freire, C. S. R., Silvestre, A. J. D., Pascoal Neto, C., Belgacem, M. N., and Gandini, A. (2006). "Controlled heterogeneous modification of cellulose fibers with fatty acids: Effect of reaction conditions on the extent of esterification and fiber properties," *J. Appl. Polym. Sci.* 100(2), 1093-1102.

Gao, H., Song, Y., Wang, Q., Han, Z., and Zhang, M. (2008). "Rheological and mechanical properties of wood fiber-PP/PE blend composites," *Journal of Forestry Research* 19(4), 315-318.

Gao, H., Xie, Y., Ou, R., and Wang, Q. (2012). "Grafting effects of polypropylene/ polyethylene blends with maleic anhydride on the properties of the resulting

wood-plastic composites," *Composites Part A: Applied Science and Manufacturing* 43(1), 150-157.

Herrera-Franco, P. J., and Valadez-González, A. (2005). "A study of the mechanical properties of short natural-fiber reinforced composites," *Composites Part B: Engineering* 36(8), 597-608.

Inari, G. N., Petrissans, M., Lambert, J., Ehrhardt, J. J., and Gérardin, P. (2006). "XPS characterization of wood chemical composition after heat-treatment," *Surface and Interface Analysis* 38(10), 1336-1342.

Lee, Y. H. (2008). "Foaming of wood flour/polyolefin/layered silicate composites," PhD Thesis, University of Toronto.

Lu, J. Z., Wu, Q., and Negulescu, I. I. (2005). "Wood-fiber/high-density-polyethylene composites: Coupling agent performance," *J. Appl. Polym. Sci.* 96(1), 93-102.

Okubo, K., Fujii, T., and Yamamoto, Y. (2004). "Development of bamboo-based polymer composites and their mechanical properties," *Composites Part A: Applied Science and Manufacturing* 35(3), 377-383.

Ou, R., and Wang, Q. (2009). "Effects of maleic rosin on the rheological properties of wood flour/HDPE composites," *Scientia Silvae Sinicae* 45(5), 126-130.

Wei, S., Shi, J., Gu, J., Wang, D., and Zhang, Y. (2012). "Dynamic wettability of wood surface modified by acidic dyestuff and fixing agent," *Appl. Surf. Sci.* 258(6), 1995-1999.

Xie, Y., Xiao, Z., Grüneberg, T., Militz, H., Hill, C. A. S., Steuernagel, L., and Mai, C. (2010). "Effects of chemical modification of wood particles with glutaraldehyde and 1,3-dimethylol-4,5-dihydroxyethyleneurea on properties of the resulting polypropylene composites," *Compos. Sci. Technol.* 70(13), 2003-2011.

Xu, H. N., Shen, Q. Y., Ouyang, X. K., and Yang, L.Y. (2012). "Wetting of soy protein adhesives modified by urea on wood surfaces," *Eur. J. Wood Wood Prod.* 70(1-3), 11-16.

Yokozeki, T., Schulz, S. C., Buschhorn, S. T., and Schulte, K. (2012). "Investigation of shear thinning behavior and microstructures of MWCNT/epoxy and CNF/epoxy suspensions under steady shear conditions," *Macromol. Nanotech.* 48(6), 1042-1049.

Zhang, S. W., Rodrigue, D., and Riedl, B. (2005). "Preparation and morphology of polypropylene/wood flour composite foams via extrusion," *Polymer Composites* 26(6), 731-738.

Zhang, Z. X., Gao, C. Y., and Xin, Z. X. (2012). "Effects of extruder parameters and silica on physico-mechanical and foaming properties of PP/wood-fiber composites," *Composites: Part B* 43(4), 2047-2057.

Zhang, Z. X., Zhang, J., Lu, B., Xin, Z. X., Kang, C. K., and Kim, J. K. (2012). "Effect of flame retardants on mechanical properties, flammability and foamability of PP/wood-fiber composites," *Composites: Part B* 43(2), 150-158.

Zhou, X. X., Lin, Q. J., and Chen, L. H. (2012). "Effects of the chemical foaming agents on mechanical properties and rheological behavior of the bamboo powder/ polypropylene foamed composite," *BioResources* 7(2), 2183-2198.

Article submitted: August 15, 2013; Peer review completed: October 9, 2013; Revised version accepted: October 14, 2013; Published: October 22, 2013.